

Spin Liquid Phase in the Pyrochlore Antiferromagnet

Benjamin Canals*

*Laboratoire Louis Néel, CNRS, 25 avenue des Martyrs,
Boîte Postale 166, 38042 Grenoble Cedex 9, France*

D. A. Garanin†

*Max-Planck-Institut für Physik komplexer Systeme,
Nöthnitzer Strasse 38, D-01187 Dresden, Germany*

(Dated: October 22, 2018)

Correlation functions (CFs) of the classical Heisenberg antiferromagnet on the pyrochlore lattice are studied by solving exactly the infinite-component spin-vector model. As in many Fully Frustrated Lattices, the constraint due to the minimization of the energy and the particular structure based on corner sharing tetrahedra both contribute to the creation of local degrees of freedom. The resulting degeneracy destroys any magnetic order at all temperature and we obtain no sign of criticality, even at $T = 0$. Calculated neutron scattering cross sections have their maxima beyond the first Brillouin Zone and reproduce experimental results obtained on $Y(\text{Sc})\text{Mn}_2$ and CsCrNiF_6 as well as theoretical predictions previously obtained by classical Monte Carlo simulations. Evidences for thermal and spatial decoupling of the magnetic modes are found so that the magnetic fluctuations in this system can be approximated by $S(q, T) \approx f(q)h(T)$.

PACS numbers: 75.10.Hk, 75.50.Ee, 75.40.Cx, 75.40.-s

I. INTRODUCTION

Motivated by the search and understanding of new quantum or classical disordered ground states in magnetic systems, recent years have seen a renewal of interest in the properties of frustrated Heisenberg antiferromagnets. Special attention focused on intrinsically frustrated models, where frustration is mainly coming from the connectivity of the underlying lattice and not only from competing interactions. From this point of view, two lattices distinguished themselves : the kagomé lattice (made of corner sharing triangles) and the pyrochlore lattice (made of corner sharing tetrahedra). Experimental and theoretical studies [1] related to both lattices have shown that materials as well as models exhibit unconventional magnetic properties, involving noncollinear or incommensurate orderings, apparently broken ergodicity without structural disorder and in general, deviations from canonical behaviors. For most geometrically frustrated systems, the absence of ordering at finite temperature or the tendency to a reduction of the real interactions seems to be a common characteristic. An experimental signature of this property is a persistent paramagnetic state down to low temperature without any sign of ordering [2]

and sometimes a transition to a frozen state at low temperature [3] ($T_F \ll |\Theta_{CW}|$), with an unconventional slowing down of the dynamics [4, 5, 6]. The theoretical understanding of these properties is in progress but it seems that several properties, expected to be generic, are not systematically reproduced and depend on the material or the model. One point is at least widely shared: due to frustration, short range correlations develop at a temperature much lower than the interactions. This phenomenon has been proven by mean field analysis [7] and classical monte-carlo simulations [8, 9, 10]. On the other hand, there are some properties much more dependent on the studied system. A major theme of study has been the effect of “order by disorder” previously quoted by Villain and co-workers [11] and also by Shender [12]. It was noticed that switching on any source of fluctuation (like thermal or quantum fluctuations) has a tendency to lift the degeneracy between the low lying classical ground states. Indeed, thermal fluctuations give rise to entropic selection in the kagomé case [13, 14] but this kind of selection was shown to be fluctuation-like dependent [15], and sometimes absent [16, 17]. Other types of perturbation have been taken into account, such as anisotropy [18], structural disorder [19], longer range interactions [7, 20] and quantum fluctuations [21, 22, 23, 24, 25, 26, 27], leading in general to a magnetic mode selection.

The pyrochlore lattice is a three dimensional arrangement of corner sharing tetrahedra as depicted in Fig. 1. According to Lacorre definition of frustration [28], it is probably the most frustrated structure. Experimentally, several families of compounds are known to crystallize

*canals@polycnrs-gre.fr; <http://ln-w3.polycnrs-gre.fr/pageperso/canals/>

†dgaranin@yahoo.com; <http://www.mpiyks-dresden.mpg.de/~garanin>

with this geometry. The first one is an oxide family with the general formula $A_2^{3+}B_2^{4+}O_7$ (Refs. 6, 29, 30) (A is a Rare Earth ion and B a transition metal). The second one concerns spinels of general formula AB_2O_4 or $A_2B_2O_4$ (Refs. 31, 32, 33) (A is a Rare Earth ion and B a transition metal). The third one concerns fluorides of general formula $AB^{2+}C^{3+}F_6$ (Refs. 34, 35) (A is an alkali metal, B and C are transition metals). The last one is the intermetallic Laves Phases compounds of general formula AB_2 (Refs. 36, 37) (A is a Rare Earth ion and B is a transition metal). Strictly speaking, the only candidate that can be rigorously described by a localized, uniform lattice model is the first family, as this system is well ordered with a uniform distribution of magnetically localized ions. The second and third sets often possess positional or chemical disorder [31, 34] that should be taken into account in the model and the last one is better described within an itinerant model [38].

In this paper, we will focus only on the isotropic classical Heisenberg model on the pyrochlore lattice, neglecting all other possible contributions that might be necessary for an understanding of a peculiar material. This choice is supported by our hope to deduce intrinsic properties which come exclusively from geometrical structure. Our goal is to compute correlation functions using an approximation of the Heisenberg model, the infinite component spin-vector model.

II. LATTICE STRUCTURE AND MODEL

The “next simplest” approximation for classical spin systems, which follows the Mean Field Approximation (MFA), consists in generalizing the Heisenberg Hamiltonian for the D -component spin vectors:

$$\mathcal{H} = -\frac{1}{2} \sum_{i,j} J_{ij} \mathbf{s}_i \cdot \mathbf{s}_j, \quad |\mathbf{s}_i| = 1 \quad (1)$$

and taking the limit $D \rightarrow \infty$. In this limit, it is possible to take into account exactly the effect of the Goldstone modes or would be Goldstone modes, which are the most important modes in frustrated magnets. We will only give the outline of the calculation here and give in a further article the details of the technique. Nevertheless, readers who are interested in the full derivation can find a description of the method in Ref. 40, where the antiferromagnetic model on the kagome lattice was considered.

The pyrochlore lattice shown in Fig. 1 consists of corner-sharing tetrahedra. Each node of the underlying Bravais lattice (face centered cubic) is numbered by $i = 1, \dots, N$ and corresponds to a tetrahedron. Each site of elementary tetrahedra is labeled by the index $l = 1, 2, 3, 4$.

It is convenient to put the Hamiltonian (1) into a diagonal form. First, one goes to the Fourier representation

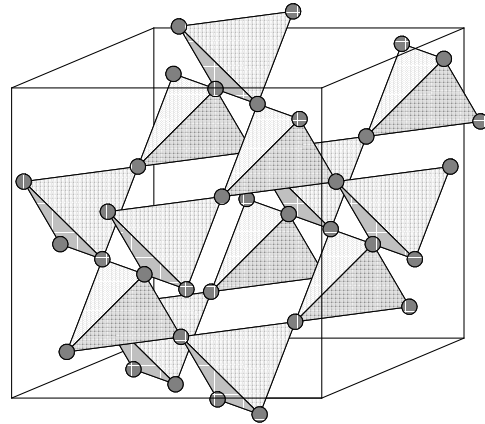


FIG. 1: Structure of the pyrochlore lattice. The elementary tetrahedra are labeled by $i = 1, \dots, N$, and the sites on tetrahedra (the sublattices) are labeled by $l = 1, 2, 3, 4$.

according to

$$\mathbf{s}_{\mathbf{q}}^l = \sum_i \mathbf{s}_i^l e^{-i\mathbf{q}r_i^l}, \quad \mathbf{s}_i^l = \frac{1}{N} \sum_{\mathbf{q}} \mathbf{s}_{\mathbf{q}}^l e^{i\mathbf{q}r_i^l}, \quad (2)$$

where the wave vector \mathbf{q} belongs to the 1st Brillouin zone of the underlying face centered cubic lattice (see Fig. 2). The Fourier-transformed Hamiltonian reads

$$\mathcal{H} = \frac{1}{2N} \sum_{l'l''} V_{\mathbf{q}}^{ll''} \mathbf{s}_{\mathbf{q}}^l \cdot \mathbf{s}_{-\mathbf{q}}^{l''}, \quad (3)$$

where the interaction matrix is given by

$$\hat{V}_{\mathbf{q}} = 2J \begin{pmatrix} 0 & b & c & a \\ b & 0 & f & d \\ c & f & 0 & e \\ a & d & e & 0 \end{pmatrix}, \quad \text{where} \quad (4)$$

$$\begin{aligned} a &\equiv \cos\left(\frac{q_y + q_z}{4}\right) & d &\equiv \cos\left(\frac{q_x - q_y}{4}\right) \\ b &\equiv \cos\left(\frac{q_x + q_z}{4}\right) & e &\equiv \cos\left(\frac{q_x - q_z}{4}\right) \\ c &\equiv \cos\left(\frac{q_x + q_y}{4}\right) & f &\equiv \cos\left(\frac{q_y - q_z}{4}\right) \end{aligned}$$

At the second stage, the Hamiltonian (3) is finally diagonalized to the form

$$\mathcal{H} = -\frac{1}{2N} \sum_{n\mathbf{q}} \tilde{V}_{\mathbf{q}}^n \sigma_{\mathbf{q}}^n \cdot \sigma_{-\mathbf{q}}^n, \quad (5)$$

where $\tilde{V}_{\mathbf{q}}^n = 2J\nu_n(\mathbf{q})$ are the eigenvalues of the matrix $V_{\mathbf{q}}^{ll''}$ taken with a negative sign,

$$\nu_{1,2} = 1, \quad \nu_{3,4} = -1 \pm \sqrt{1+Q}. \quad (6)$$

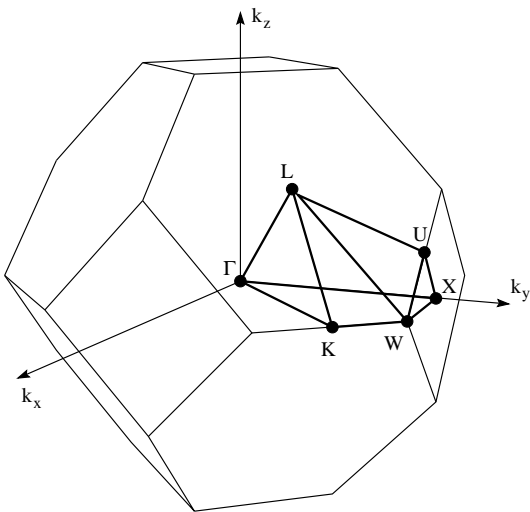


FIG. 2: Brillouin zone of the pyrochlore lattice. Letters Γ , X , W , U and L are high symmetry points using the usual crystallographic conventions.

where

$$Q = \frac{1}{2} \left(\cos\left(\frac{q_y + q_z}{2}\right) + \cos\left(\frac{q_x + q_z}{2}\right) + \cos\left(\frac{q_x + q_y}{2}\right) + \cos\left(\frac{q_x - q_y}{2}\right) + \cos\left(\frac{q_x - q_z}{2}\right) + \cos\left(\frac{q_y - q_z}{2}\right) \right) \quad (7)$$

The diagonalizing transformation has the explicit form

$$U_{nl}^{-1}(\mathbf{q}) V_{\mathbf{q}}^{ll'} U_{l'n'}(\mathbf{q}) = \tilde{V}_{\mathbf{q}}^n \delta_{nn'}, \quad (8)$$

where the summation over the repeated indices is implied and \hat{U} is the real unitary matrix, $\hat{U}^{-1} = \hat{U}^T$, i.e., $U_{nl}^{-1} = U_{ln}$.

The Fourier components of the spins $\mathbf{s}_{\mathbf{q}}^l$ and the collective spin variables $\sigma_{\mathbf{q}}^n$ are related by

$$\mathbf{s}_{\mathbf{q}}^l = U_{ln}(\mathbf{q}) \sigma_{\mathbf{q}}^n, \quad \sigma_{\mathbf{q}}^n = \mathbf{s}_{\mathbf{q}}^l U_{ln}(\mathbf{q}). \quad (9)$$

The largest dispersionless eigenvalues $\nu_{1,2}$ of the interaction matrix [see Eq. (6) and Fig. 3] are a manifestation of frustration in the system which precludes an extended short-range order even in the limit $T \rightarrow 0$. Since $\nu_{1,2}$ are independent of \mathbf{q} , $1/2$ of all spin degrees of freedom are local and can rotate freely. The eigenvalue ν_3 which becomes degenerate with $\nu_{1,2}$ in the limit $q \rightarrow 0$ is related, to the usual would be Goldstone mode destroying the long-range order in low-dimensional magnets with a continuous symmetry whereas the eigenvalue ν_4 is positioned, in the long-wavelength region, much lower than the first two ones, and it is tempting to call it the “optical” eigenvalue.

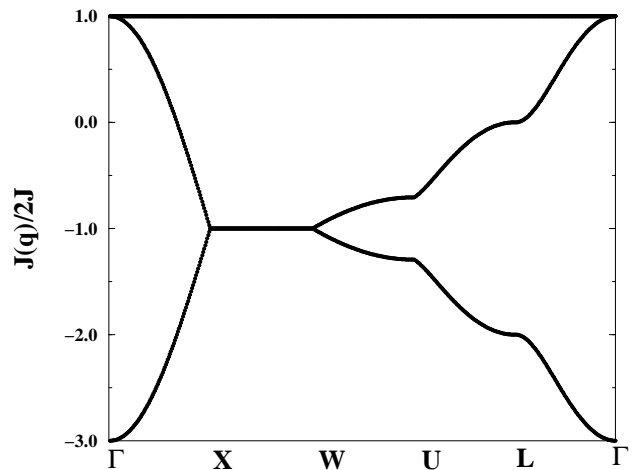


FIG. 3: Reduced eigenvalues of the interaction matrix, $\nu_n(\mathbf{q}) = \tilde{V}_{\mathbf{q}}^n / (2J)$ of Eq. (5). They are plotted such that they cover the high symmetry axis of the face centered cubic Brillouin Zone (see Fig. 2).

III. RESULTS

Following the derivation introduced in Ref. 40, we compute all CF’s at any temperature and in particular, the static magnetic neutron scattering cross section :

$$\frac{d\sigma}{d\Omega} \propto \sum_{\mathbf{r}\mathbf{r}'} \langle S_{\mathbf{r}}^{\perp} S_{\mathbf{r}'}^{\perp} \rangle e^{i\mathbf{Q}(\mathbf{r}-\mathbf{r}')}, \quad (10)$$

where \mathbf{Q} is a vector of the reciprocal space and r and r' design spin belonging to the pyrochlore lattice, i.e., $S_{\mathbf{r}} = S_i^l$ is a spin located on site i of the Bravais lattice in the position l of the unit cell. Two peculiar planes of the reciprocal space have been investigated as shown in Fig. 4 and Fig. 5. The major feature is that there is almost no magnetic signal in the first Brillouin zone, all the weight being recovered in soft cusps outside. In both planes, we observe patterns very similar to the one obtained by Monte Carlo simulations in Ref. 39 or by neutron diffraction on $Y(\text{Sc})\text{Mn}_2$ [2]. We also note that the cross section in the $([\text{hh}0], [001])$ plane is very close to the one previously calculated in the kagome case by the same method [40]. The main implications of these results are that the quantum or classical nature of the spins in the pyrochlore lattice does not seem to be of relevance for understanding the liquid nature in terms of spin-spin correlations. Indeed, different methods and measures, applied to different spin species (classical or quantum), give the same magnetic responses. Besides, the very strong resemblance between the neutron diffraction pattern in the $([\text{hh}0], [001])$ plane and the one obtained in the kagome antiferromagnet is evidence that these two lattices are very similar. This is not surprising as the kagome lattice is a cut of the pyrochlore lattice perpendicular to the (111) axis. As previously noted in Ref. 21 there are two magnetic modes coexisting in this system (see Fig.

4 and Fig. 5). The one related to the $([hh0],[00l])$ plane ($Q_1 = [220] \pm [\frac{3}{4}\frac{3}{4}0]$ or $Q'_1 = [002] \pm [\frac{3}{4}\frac{3}{4}0]$) would coincide in an ordered phase with a structure where consecutive tetrahedra are in phase, while the one in the $([h00],[010])$ plane ($Q_2 = [210]$) correspond to a π phase between tetrahedra. Whereas in the quantum approach[21] there is a difference of amplitude between these two modes, within our approach both have the same amplitude so that the system is unable to select a particular one. The powder average of the neutron cross section $\langle d\sigma/d\Omega \rangle$, i.e., the average of 10 over the directions of q is shown in Fig. 6. The continuous line is obtained from the $D = \infty$ component classical antiferromagnet approach while the dots correspond to Monte Carlo simulations performed in Ref.41. There is a good agreement between these two methods and they do not show any sign of magnetic transition. We have calculated the effect of the temperature on the powder average cross section. In Fig. 7 we have plotted the variation of the profiles with reduced temperature ($\theta = T/T_{\text{MFA}}$ where $T_{\text{MFA}} = 2J/3$). One can see that at temperature below T_C^{MFA} , i.e., below $\theta = 1$, these profiles have approximately the same shape. In order to control that quantity, we have rescaled each profile and plotted them one onto the others. As they almost coincide, it means that at low temperature we can decouple the q dependence and the θ dependence so that $\langle d\sigma/d\Omega \rangle(Q, \theta) \approx \langle d\sigma/d\Omega \rangle(Q, \theta = 0)f(\theta)$. The same type of decoupling was assumed in Ref. 21 where the authors proposed that the spatial and the time dependence could be independent at low temperatures ($\chi(q, \omega) \approx f(q)g(\omega)$). These properties are original and certainly come from the high frustration of the pyrochlore lattice and its related dynamics. At first approximation, we can state that spatial and time as well as spatial and thermal dependence are decoupled at energy scales lower than the mean field temperature.

IV. DISCUSSION

In this article, we have presented the structure of the neutron diffraction cross sections obtained from the exact solution for the $D = \infty$ component classical antiferromagnet on the pyrochlore lattice.

In contrast to conventional three dimensional magnets, there is no ordering and even no extended short range order at $T = 0$. This anomalous behavior is due to the existence of a would be Goldstone mode at low temperature but also to the presence of two dispersionless excitations modes that inhibit any magnetic transition.

The magnetic cross sections are very close to what has been obtained in theoretical approaches (Monte Carlo simulations with Heisenberg spins [39], density matrix expansion for spin $S = 1/2$ [21]) and experimental results (Y(Sc)Mn₂ [2], CsNiCrF₆ [34, 35]). We have reproduced the existence of two dominant magnetic modes that could explain a first order transition induced by magnetoelastic effects [2]. It is remarkable that the nature of the

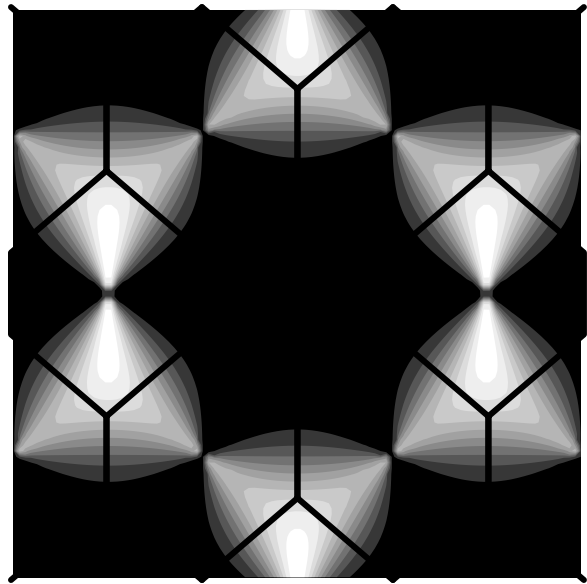


FIG. 4: Neutron scattering cross section from the large- D pyrochlore antiferromagnet at $T = 0$ in the $([hh0],[00l])$ plane. (cf. Fig. 2). Dark regions are low intensity ones while white regions correspond to the maximum of the scattering.

spins (classical or quantum) as well as the type of magnetism (localized or itinerant) does not seem to play a crucial role in the pyrochlore system. Even the geometry, three dimensional here, seem to have a very little effect on the structure of the magnetic response. In fact, we obtain results similar to the ones previously observed on the kagome lattice. Even if this point is not solved, it is clear that the close relation between these two lattices, and the short range scale of the geometry are the relevant ingredients in the pyrochlore and the kagome antiferromagnets.

Taking into account assumptions of Ref.21 we can say that spatial and thermal as well as spatial and time dependences of the magnetic cross sections are decoupled at low energy scale (i.e. $T \lesssim J$) as if $S(q, T) \approx f(q)h(T)$ and $S(q, \omega) \approx f(q)g(\omega)$. This striking result confirms that this model describes an unconventional antiferromagnet and has some similarities with a collective paramagnet.

All these points strongly support that isotropic antiferromagnetic Heisenberg models (quantum or classical) on the pyrochlore lattice are spin liquids.

Although this point is now clearer, it is still an open problem to understand the experimental results that suggest the appearance of a topological spin glass like behavior. There must certainly be other interactions or processes involved in this case as up to now, no sign of glassiness has ever been seen within theoretical approaches concerning the Heisenberg model on the pyrochlore lattice.

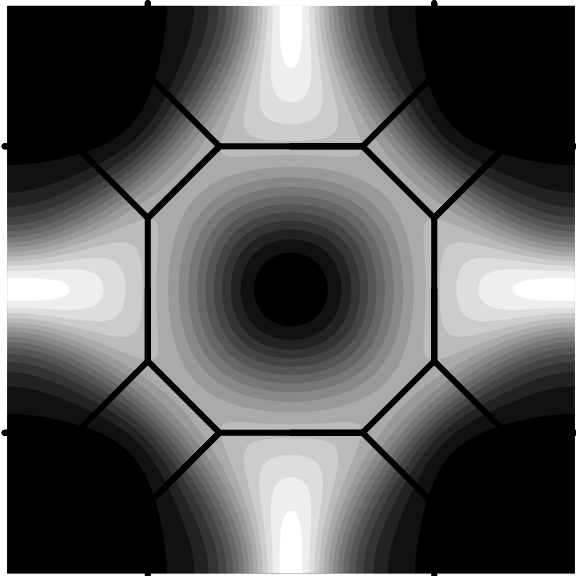


FIG. 5: Neutron scattering cross section from the large- D pyrochlore antiferromagnet at $T = 0$ in the $([h00],[010])$ plane. (cf. Fig. 2). Dark regions are low intensity ones while white regions correspond to the maximum of the scattering.

REFERENCES

- [1] For a collection of articles, see *Magnetic systems with Competing Interactions : Frustrated Spin System*, edited by H. T. Diep (World Scientific, Singapore, 1994); for Ising systems, see R. Liebmann, *Statistical Mechanics of Periodic Frustrated Ising Systems* (Springer, Berlin, 1986); for reviews, see A. P. Ramirez, *Annu. Rev. Mater. Sci.* **24**, 453, (1994); P. Schiffer and A. P. Ramirez, *Comments Cond. Mat. Phys.* **18**, 21, (1996); M. J. Harris and M. P. Zinkin, *Mod. Phys. Lett. B* **10**, 417, (1996).
- [2] R. Ballou, E. Lelièvre-Berna and B. Fåk, *Phys. Rev. Lett.* **76**, 2125, (1996).
- [3] M. J. P. Gingras, C. V. Stager, N. P. Raju, B. D. Gaulin and J. E. Greedan, *Phys. Rev. Lett.* **78**, 947, (1997).
- [4] Y. J. Uemura, A. Keren, L. P. Le, G. M. Luke, B. J. Sternlieb and W. D. Wu, *Hyperfine Interact.* **85**, 133 (1994).
- [5] Y. J. Uemura, A. Keren, K. Kojima, L. P. Le, G. M. Luke, W. D. Wu, Y. Ajiro, T. Asano, Y. Kuriyama, M. Mekata, H. Kikuchi and K. Kakurai, *Phys. Rev. Lett.* **73**, 3306 (1994).
- [6] S. R. Dunsiger, R. F. Kiefl, K. H. Chow, B. D. Gaulin, M. J. P. Gingras, J. E. Greedan, A. Keren, K. Kojima, G. M. Luke, W. A. MacFarlane, N. P. Raju, J. E. Sonier, Y. J. Uemura, and W. D. Wu, *Phys. Rev. B* **54**, 9019 (1996).
- [7] J. N. Reimers, A. J. Berlinsky and A.-C. Shi., *Phys. Rev. B* **43** (1991) 865.
- [8] J. N. Reimers, J. E. Greedan, and M. Björgvinsson, *Phys. Rev. B* **45**, 7295 (1992).
- [9] J. N. Reimers, *Phys. Rev. B* **45**, 7287 (1992).
- [10] R. Moessner and J. T. Chalker, *Phys. Rev. Lett.* **80**, 2929 (1998); R. Moessner and J. T. Chalker, *Phys. Rev. B* **58**, 12049 (1998).
- [11] J. Villain, R. Bidaux, J. P. Carton, R. Conte, J. *Phys.* **41**, 1263 (1980).
- [12] E. F. Shender, *Sov. Phys.-JETP*, **56**, 178 (1982).
- [13] J. T. Chalker, P. C. W. Holdsworth and E. F. Shender, *Phys. Rev. Lett.* **68**, 855 (1992).
- [14] I. Ritchey, P. Chandra and P. Coleman, *Phys. Rev. B* **47**, 15342 (1993).
- [15] B. Douçot and P. Simon, *J. Phys. A: Math. Gen.* **31**, 5855 (1998).
- [16] D. A. Huse and A. D. Rutenberg, *Phys. Rev. B* **45**, 7536 (1992).
- [17] P. Chandra and B. Douçot, *J. Phys. A*, **27**, 1541 (1994).
- [18] S. T. Bramwell, M. J. P. Gingras, and J. N. Reimers, *J. Appl. Phys.* **75**, 5523 (1994).
- [19] E. F. Shender, V. B. Cherepanov, P. C. W. Holdsworth and A. J. Berlinsky, *Phys. Rev. Lett.* **70**, 3812 (1993).
- [20] A. B. Harris, C. Kallin and A. J. Berlinsky, *Phys. Rev. B* **45**, 2899 (1992).
- [21] B. Canals and C. Lacroix, *Phys. Rev. Lett.* **80**, 2933 (1998); B. Canals and C. Lacroix, *Phys. Rev. B* **61**, 1149 (2000).
- [22] R. R. Sobral and C. Lacroix, *Solid State Comm.* **103**, 407 (1997).
- [23] A. B. Harris, A. J. Berlinsky and C. Bruder, *J. Appl. Phys.* **69**, 5200 (1991).
- [24] J. B. Marston and C. Zeng, *J. Appl. Phys.* **69**, 5962 (1991).
- [25] S. Sachdev, *Phys. Rev. B* **45**, 12377 (1992).

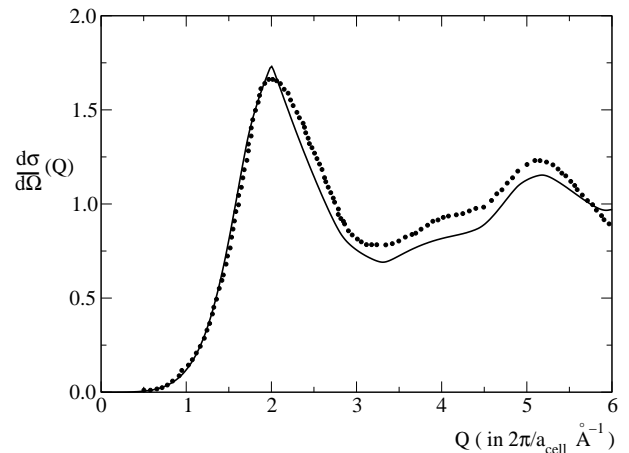


FIG. 6: Powder average of the neutron scattering cross section from the pyrochlore antiferromagnet. The straight line correspond to the $T = 0$ case in the $D = \infty$ component classical antiferromagnet approach while dots are extracted points from the Monte Carlo results obtained in Ref.41

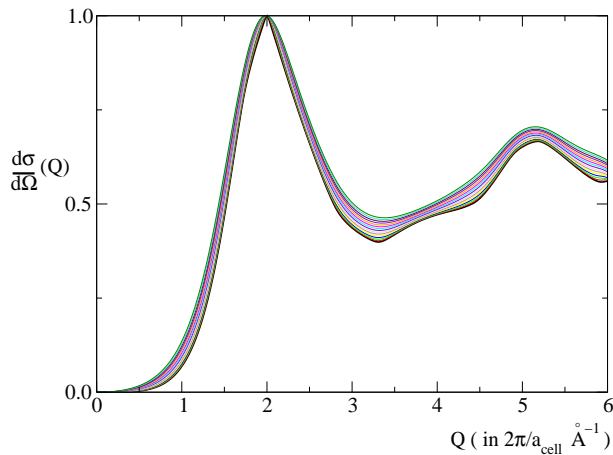


FIG. 7: Powder average of the neutron scattering cross section from the pyrochlore antiferromagnet at different temperatures ($\theta \in [0, 1]$). Each curve is rescaled to be compared with the $T = 0$ one.

- [26] A. Chubukov, Phys. Rev. Lett. **69**, 832 (1992).
 [27] P. Lecheminant, B. Bernu, C. Lhuillier, L. Pierre and P. Sindzingre, Phys. Rev. B **56**, 2521 (1997).
 [28] P. Lacorre, J. Phys. C: Solid State Phys. **20**, L775, (1987).
 [29] J. S. Gardner, S. R. Dunsiger, B. D. Gaulin, M. J. P. Gingras, J. E. Greedan, R. F. Kiefl, M. D. Lumsden, W. A. MacFarlane, N. P. Raju, J. E. Sonier, I. Swainson, and Z. Tun, Phys. Rev. Lett. **82**, 1012 (1999).
 [30] J. E. Greedan, J. N. Reimers, C. V. Stager, and S. L. Penny, Phys. Rev. B **43**, 5682 (1991); J. N. Reimers, J. E. Greedan, C. V. Stager, M. Bjorgvinssen, and M. A. Subramanian, *ibid* **43**, 5692 (1991).
 [31] A. S. Wills, N. P. Raju, and J. E. Greedan, Chem. Mater. **11**, 1510 (1999).
 [32] J. E. Greedan, N. P. Raju, A. S. Wills, C. Morin, and S. M. Shaw, Chem. Mater. **10**, 3058 (1998).
 [33] N. Fujiwara, H. Yasuoka, and Y. Ueda, Phys. Rev. B **57**, 3539 (1998).
 [34] M. J. Harris and M. P. Zinkin, and T. Zeiske, Phys. Rev. B **56**, 11786 (1997).
 [35] M. J. Harris, M. P. Zinkin, Z. Tun, B. M. Wankly and I. P. Swainson, Phys. Rev. Lett. **73**, 189, (1994).
 [36] M. Shiga, J. Magn. Magn. Mater. **129**, 17 (1994).
 [37] M. Shiga, Physica B **149**, 293 (1988).
 [38] R. Ballou, C. Lacroix, and M. D. Nunez-Regueiro, Phys. Rev. Lett. **66**, 1910 (1996).
 [39] M. P. Zinkin, M. J. Harris, T. Zeiske, Phys. Rev. B **56**, 11786, (1997).
 [40] D. A. Garanin and B. Canals, Phys. Rev. B **59**, 443 (1999).
 [41] J. N. Reimers, Phys. Rev. B **46**, 193 (1992).